International Journal of Multiphysics
Volume 18, No. 3, 2024
ISSN: 1750-9548

Analytical and Numerical Study of Temperature Distribution in Functionally Graded Fins

Adnan A. Hussein[1, a] Nasr A. Jabbar [1, b], Muna Hameed Alturaihi [1, c]Sahib S. Ahmed [1, d], Luay S. Al-Ansari[1, e]

[1] University of Kufa, Faculty of Engineering, Department of Mechanical Engineering, Kufa, Najaf, Iraq.
[a] adnana.alzaheri@uokufa.edu.iq, [b] nasra.hamood@uokufa.edu.iq, [c] monah.alturaihi@uokufa.edu.iq
[d] sahib.aldulaimi@uokufa.edu.iq, [e] luays.alansari@uokufa.edu.iq

Abstract:
This work investigates heat conduction in a functionally graded Fin subjected to gradual cooling/heating at its boundaries analytically and numerically. It is assumed that the thermal properties of the functionally graded material are coordinated changes in the fin length direction. The linear model is applied to determine the physical properties of the functionally graded materials. To analyze the thermal behavior of the heat sink, two approximate analytical methods are used: first, the method relies on the mean value theorem. The second method relies on the principle of equivalent properties. The Numerical solution carried by ANSYS APD depends on stepped variation of properties. The results showed that the factor of property ratio controls temperature levels where the temperature levels at the end of the functionally graded fin change exponentially with the factor of property ratio. The effect of functionally graded material starts within the length where the maximum effect appears at the fin's end. The maximum absolute error percentage between the analytical and numerical results is (6.756%), which means a good match between both solutions.

Keyword: Rectangular fin, Mean value theorem, Functionally Graded Material, Temperature distribution, Heat sink.

1. Introduction:

The utilization of overtime fins in heat transfer equipment has become advantageous owing to their comparatively expansive surface area, which amplifies heat transfer. Consequently, it functions as a highly efficient heat transfer medium in various applications, including but not limited to automobiles, steam power plants, furnaces, air conditioning and refrigeration devices, and more. Extensive scientific and engineering research has been devoted to the investigation, analysis, and experimental examination of fins, which are of the utmost importance [1].

In recent years, functionally graded material (FGM) has emerged as a novel material development. It is distinguished by the fact that the material's composition exhibits a continuous gradient change in the direction of thickness. Additionally, the material's characteristics and function exhibit a gradient change. Additionally, the thermal and residual stresses of the material can be mitigated. When juxtaposed with conventional materials, the characteristics of FGM exhibit a substantial enhancement. Owing to its exceptional physical characteristics, it was found that it is extensively applicable in many high-temperature environment applications. Analyzing the heat conduction and temperature distribution characteristics is thus particularly crucial [2]. In recent years, many scholars have investigated the heat conduction of FGM, concentrating primarily on the analytical and numerical methods [3]. Gaba et al. [4] introduced an analytical solution to study annular fins with constant weight from FGM. A comprehensive second-order governing differential equation has been formulated to analyze the variation in material thickness and thermal conductivity along a given radius for all profiles and material grading. Oguntala et al. [5] resolved thermal models by utilizing the Chebyshev spectral collocation method, which postulated that the thermal properties of the functionally graded material followed a linear and power-law function. This study investigates the impact of convective and radiative parameters and the inhomogeneity index of FGM on the thermal behavior of a porous heat sink. Khan et al. [6] derived an analytical solution to analyze the performance of a steady case of the fin in terms of Bessel functions when thermal conductivity with longitudinal length is linear and exponential, as well as Legendre functions for the quadratic case. The fin's transient and steady-state performance is found to be substantially influenced by the functional classification of the fin material. The thermal properties of materials utilized in heat exchangers with FGM longitudinal fins were evaluated by Hassazadeha and Bilgib [7]. The resultant equations were computed while two boundary conditions (Dirichlet and Neumann) were applied. An approximation analytical method was utilized to resolve the equations by employing the mean value theorem. In such heat exchangers, the results demonstrated that the inhomogeneity index of a functionally graded material significantly influences the thermal energy characteristics. Jemiseye et al. [8] used a Numerical model and analytical solution by Laplace Transformation-Legendre wavelet collocation methods to scrutinize the thermal responses of the functionally graded rectangular fin. When subjected to quadratic heat conductivity, the passive device exhibited improved thermal distribution and a lower fin temperature than those with linear and exponential heat conductivities. Sobamowo et al. [9] presented a nonlinear transient thermal analysis of a convective-radiative fin containing functionally graded materials (FGMs) under the influence of a magnetic field. Approximate and analytical solutions were obtained for nonlinear thermal models representing linear, quadratic, and exponential variations in thermal conductivity through the differential transformation method (DTM). The findings indicated that enhancing the inhomogeneity index radiative and magnetic field parameters contributed to the improved thermal performance of the fin. In addition, the FGM fin with quadratic and exponential law functions exhibited the slowest and quickest thermal responses, respectively, as determined by the transient responses. Hassanzadeh and Bilgili [10] employed a rough analytical method predicated on the mean value theorem to assess the heat sink's thermal performance. The findings of this investigation demonstrate that substituting the material used for the fins of heat sinks with functionally graded material results in substantial energy conservation for heat sinks due to enhanced heat transmission between the fin surfaces and the surrounding fluid. Ranjana and Mallicka [11] utilized an approximate analytical approach, and the homotopy perturbation method, the nonlinear dimensionless equation for a functionally graded material's conductive-convective-radiative annular fin, was solved. In addition, a numerical model was used to verify the results. An overall investigation of thermal performance is carried out, where the effect of some factors such as thermo-geometric, conduction—radiation, thermal conductivity variation, heat generation, exponent of heat transfer coefficient, and the parameter of surface emissivity was significant on heat transfer rate, efficiency, effectiveness, and temperature distributions. George et al. [12] utilized the differential transform method, and the impacts of the nonhomogeneous index of functionally graded material, convective, and radiative parameters on the thermal performance of a porous heatsink were investigated. To forecast the heat transmission of the undulating porous fin, a hybrid model integrating the artificial neural network (ANN) and the differential evolution (DE) algorithm was put forth by Kumar et al. [13]. This study examined the significance of some parameters on the temperature field and the heat transfer rate graphically. Oguntala et al. [14] investigated the impact of Lorentz force on the longitudinal fin performance of functionally graded material. In that order, Bessel, Legendre, and modified Bessel functions were utilized to solve the governing equations of the linear, quadratic, and exponential functions, respectively. The thermal properties of the fin exhibited enhancement as the convective, radiative, magnetic field parameter, and nonhomogeneous index were all increased. Furthermore, the energy-saving capability of the power law function was considerably greater than that of the linear class functionally graded material radiator. A finite element analysis was presented by Sobamowo et al. [15] to examine the transient thermal response of a convective-radiative fin composed of functionally graded material when subjected to a temperature-varying magnetic field. The parametric studies revealed that the temperature of the extended surface increases in the same order as the homogeneity index. Also, the augmentations of the radiation and magnetic field parameters lead to a decrease in the thermal distribution of the extended surface, which consequently increases the heat transfer rate through the passive device.

In this paper, an analytical and numerical solution is presented. The 1-dimensional axial FGM-based fin is used to study the effect of these materials on the temperature distribution of FG-based fins, assuming a linear model to describe the thermal properties of the FG fins. In addition, the equivalent properties model is compared with the linear model and the numerical work of ANSYS APDL. The results of the numerical model were compared with the analytical solution to expand the study's scope and increase the work's reliability.

2. Problem Description:

As shown in Figure (1), a fin of length (L), width (w), and thickness (t) has two faces of dimensions (L*w) exposed heat transfer convection. Its base temperature is constant (T_b). This fin is made of Functionally graded materials (FGMs).

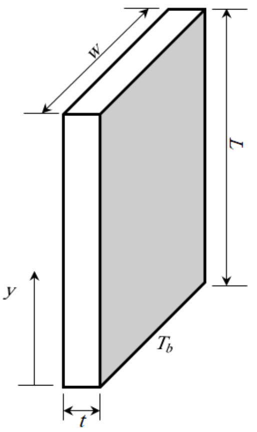

Figure (1): Dimensions of Fin.

Functionally graded materials (FGMs) are new materials with desired mechanical and thermal properties distribution. The distribution of material properties can be achieved in 1-dimension, 2-dimension, and 3-dimensions of FG directions. In 1-dimensional FGMs, various models or equations, including the power-law model, are employed to characterize the distribution of material properties in FGMs, exponential, and sigmoid models [16]. In this work, the 1-dimension axial FGMs are used to study the impact of these materials on the temperature levels distribution of FG Fins, assuming a linear model to describe the thermal properties of FG Fins as shown in equation (1):

$$P(y) = P_0 * (1 + f * \tau * y) \qquad \ldots(1)$$

$P(y)$ – The property at any point (y).

P_0– The property at point (y=0).

τ– The slop of linear equation ($\tau = \frac{P(0)}{P(L)} - 1$).

f– Factor of property ratio (Property Ratio $= \frac{P(0)}{P(L)}$).

L– Length of fin.

The material properties along the fin length are illustrated in Figure (2), and the material properties of the two parents of FGM are listed in Table (1). The slope of linear equation (τ) is constant in this case because the property ratio ($\frac{P(0)}{P(L)}$) is constant.

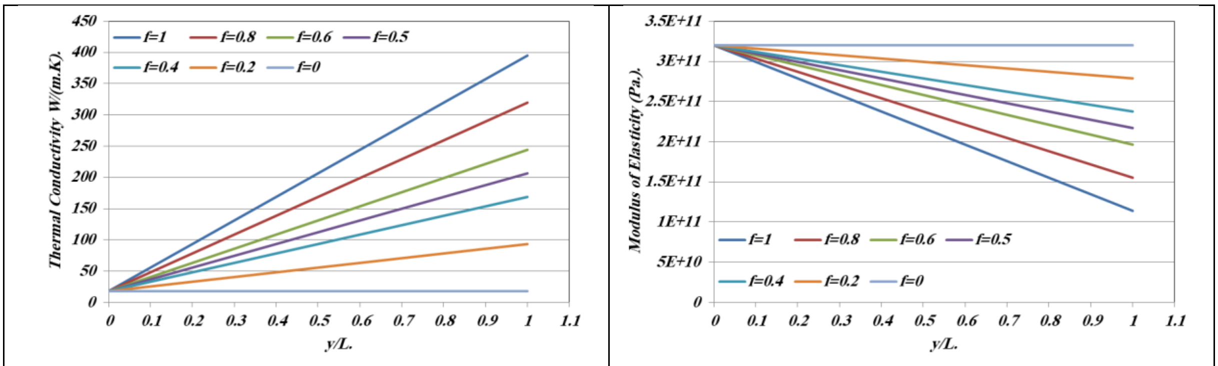

(a) Thermal Conductivity. (b) Modulus of Elasticity.

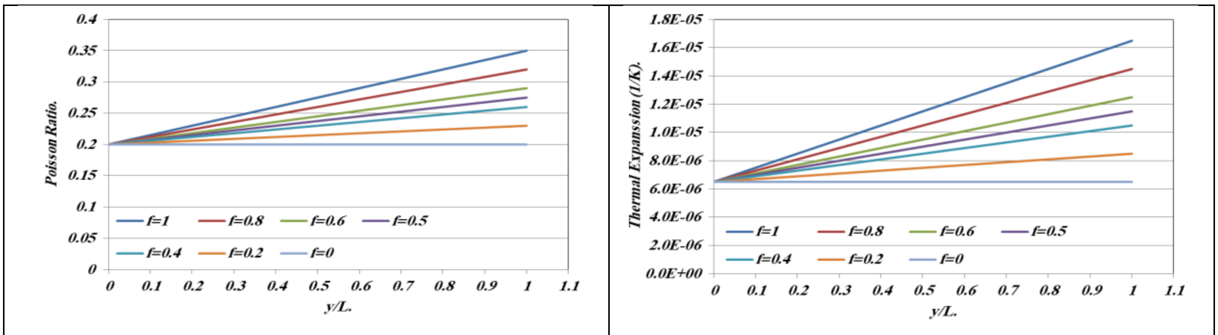

(c) Poisson Ratio.	(d) Thermal Expansion.

Figure (2): Material Properties of Linear FG Fin When the parent materials are Alumina (Al_2O_3) and Copper (Cu).

Table (1): Material Properties of the Two Parents of FGM (Alumina- Copper) [17]			
Property	***Unit***	***Alumina (Al2O3)***	***Copper (Cu)***
Poisson Ratio	***----***	***0.2***	***0.35***
Modulus of Elasticity	***GPa.***	***320***	***114***
Thermal Conductivity	***W/(m.K).***	***18***	***395***
Thermal Expansion	***1/K***	***$6.5*10^{-6}$***	***$16.5*10^{-6}$***

3. Mathematical Model:

In this work, two new models are proposed to simulate the heat transfer problem of FG fin. The first is the analytical model, while the second is the numerical model. The finite element method is applied to create the numerical model, and the ANSYS APDL software is utilized to simulate the heat transfer problem of the FG fin.

a-) Analytical Solution:

Figure (3) shows the geometry of the FG fin with a constant base temperature (T_b) and the heat convection at the two surfaces of the FG fin (L*w). From Figure (3), the heat conduction through the FG fin equals the heat convection from the fin's surfaces, and the governing equation is [18]:

$$\frac{d}{dy}\left(k\frac{dT}{dy}\right) = \frac{h}{t}(T - T_\infty) \quad 0 \le y \le L \qquad \ldots(2)$$

The boundary conditions are:

(i) at y=0 $\rightarrow T = T_b$.

(ii) at y=L $\rightarrow \frac{dT}{dy} = 0$.

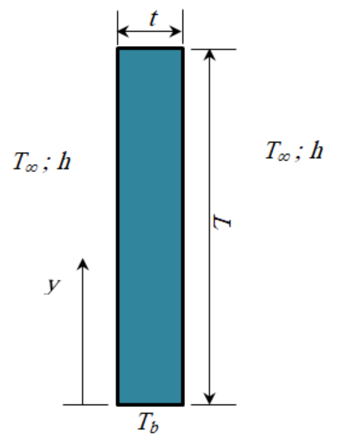

Figure (3): Geometry and Boundary Conditions of FG Fin.

From Equation (1), the thermal conductivity can be written as:
$k(y) = k_0 * (1 + f * \tau * y)$ …(3)
And equation (2) becomes:
$\frac{d}{dy}\left(k_0 * (1 + f * \tau * y)\frac{dT}{dy}\right) = \frac{h}{t}(T - T_\infty)$ …(4)

In order to solve the governing equation of the problem(i.e. Equation (4)), let; $\theta = \frac{T-T_\infty}{T_b-T_\infty}$ and $\eta = \frac{y}{L}$, therefore, $d\theta = \frac{dT}{T_b-T_\infty}$ and $d\eta = \frac{dy}{L}$. By using Chain Rule, Equation (4) and boundary conditions become:

$$(1 + f\tau\eta)\frac{d^2\theta}{d\eta^2} + f\tau\frac{d\theta}{d\eta} = \frac{hL^2}{tk_0}\,\theta$$

$$(1 + f\tau\eta)\frac{d^2\theta}{d\eta^2} + f\tau\frac{d\theta}{d\eta} - \frac{hL^2}{tk_0}\,\theta = 0$$

$(1 + f\tau\eta)\frac{d^2\theta}{d\eta^2} + f\tau\frac{d\theta}{d\eta} - \Gamma^2\,\theta = 0$ …(5)

Where : $\Gamma^2 = \frac{hL^2}{tk_0}$
The boundary conditions are:
(i) at η=0 $\rightarrow T = T_b \rightarrow \theta = 1$
(ii) at η=1 $\rightarrow \frac{dT}{dy} = 0 \rightarrow \frac{d\theta}{d\eta} = 0$.

Substituting $\eta = 0.5$ [19] at equation (5):
$(1 + 0.5f\tau)\frac{d^2\theta}{d\eta^2} + f\tau\frac{d\theta}{d\eta} - \Gamma^2\,\theta = 0$ …(6)
The solution of equation (6) is:
$\theta(\eta) = c_1 e^{\mu_1\eta} + c_2 e^{\mu_2\eta}$ …(7)
Where: $\mu_{1,2} = \frac{-(f\tau)\mp\sqrt[2]{(f\tau)^2-4(1+0.5f\tau)\Gamma^2}}{2*(1+0.5f\tau)}$
To find the values of (c_1) and (c_2), the boundary conditions are applied and :
$c_1 = \frac{\frac{\mu_2}{\mu_1}e^{\mu_2-\mu_1}}{\left(\frac{\mu_2}{\mu_1}e^{\mu_2-\mu_1}-1\right)}$ and $c_2 = \frac{1}{\left(1-\frac{\mu_2}{\mu_1}e^{\mu_2-\mu_1}\right)}$
$\therefore \theta(\eta) = \frac{\frac{\mu_2}{\mu_1}e^{\mu_2-\mu_1}}{\left(\frac{\mu_2}{\mu_1}e^{\mu_2-\mu_1}-1\right)}e^{\mu_1\eta} + \frac{1}{\left(1-\frac{\mu_2}{\mu_1}e^{\mu_2-\mu_1}\right)}e^{\mu_2\eta}$ …(8)
$\therefore T(\eta) = T_\infty + \left[(T_b - T_\infty) * \left(\frac{\frac{\mu_2}{\mu_1}e^{\mu_2-\mu_1}}{\left(\frac{\mu_2}{\mu_1}e^{\mu_2-\mu_1}-1\right)}e^{\mu_1\eta} + \frac{1}{\left(1-\frac{\mu_2}{\mu_1}e^{\mu_2-\mu_1}\right)}e^{\mu_2\eta}\right)\right]$ …(9)
For the homogenous fin, $\tau = 0$, this leads to the following:
$\frac{d^2\theta}{d\eta^2} + -\Gamma^2\,\theta = 0$ …(6')
$\theta(\eta) = c_1 e^{\mu_1\eta} + c_2 e^{\mu_2\eta}$ …(7')
Where: $\mu_{1,2} = \mp\Gamma$
Also;
$c_1 = \frac{e^{-2\Gamma}}{(1+e^{-2\Gamma})}$ and $c_2 = \frac{1}{(1+e^{-2\Gamma})}$

$\therefore T(\eta) = T_\infty + \left[(T_b - T_\infty) * \left(\frac{e^{-2\Gamma}}{(1+e^{-2\Gamma})}e^{\mu_1\eta} + \frac{1}{(1+e^{-2\Gamma})}e^{\mu_2\eta}\right)\right]$ …(9')

b-) Numerical Model:

The numerical model is built using ANSYS APDL software and using the tetrahedral element with ten nodes (SOLID87) [20]. The suitable size of a tetrahedral element is chosen depending on convergent criteria of numerical solution. The numerical model is achieved according to the following steps:

(1) Drawing the FG fin: The FG fin is divided into ten parts [21], and the used dimensions of the FG fin are listed in Table (2). The dimensions of each part are (L/10) length, (w) width, and (t) thickness (see Figure (4-a)).

(2) Material Properties: Each part of the FG fin is assumed to be a homogenous material using the following equation. The material properties of each component are computed as:

$$P_i = \frac{\left(P(i*DL)+P((i-1)*DL)\right)}{2} \qquad i = 1,2, \ldots..10 \qquad \ldots(10)$$

Where: P_i Is the property of the i-th part of FG Fin, and (DL) is the length of each part of FG Fin (see Table (2)). This model inserts ten sets of material properties into ANSYS APDL Software.

(3) Boundary Conditions: Three boundary conditions are applied in this numerical model. The first one is "applying constant temperature at the base surface of FG fin" (see Figure (3)). The second boundary condition is applied by considering an insulated fin's tip. "free convection at two surfaces of each part of FG fin is the third boundary condition by assuming constant heat convection coefficient (h-constant) and constant surrounding temperature (T∞- constant)".

(4) Solving the Numerical Model: The steady state heat transfer problem is considered in this model.

(5) Results: To investigation the effect of material properties difference of FG fin on the temperature levels distribution. The temperature distribution at the FG fin's center and the FG fin's length are drawn.

Table (2) Dimensions of FG Fin and Parts		
Dimension	***Value***	***Unit***
Length of FG Fin (L)	***0.1***	***m***
Width of FG Fin (w)	***0.04***	***m***
Thickness of FG Fin (t)	***0.003***	***m***
No. of Division of FG Fin	***10***	
Length of each part of FG Fin (DL)	***0.005***	***m***
Width of each part of FG Fin (w)	***0.04***	***m***
Thickness of each part of FG Fin (t)	***0.003***	***m***

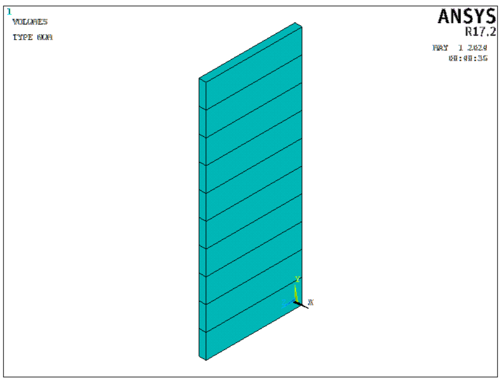

(a) Drawing FG Fin.

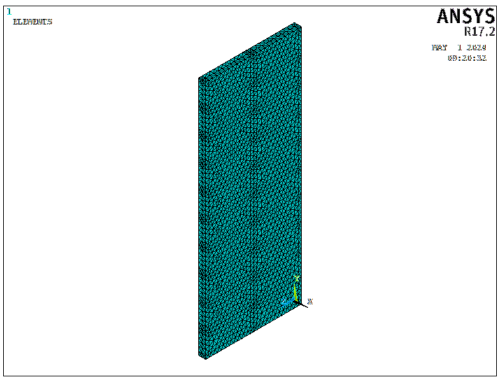

(b) Meshing the Model.

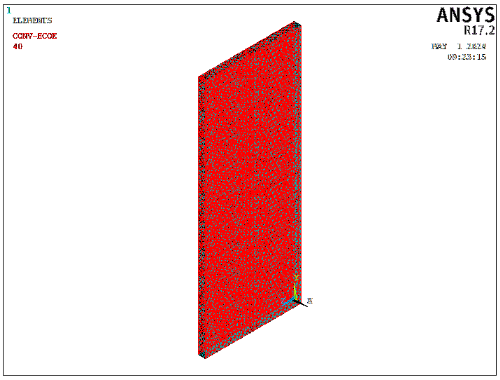

(c) Applying Boundary Condition.

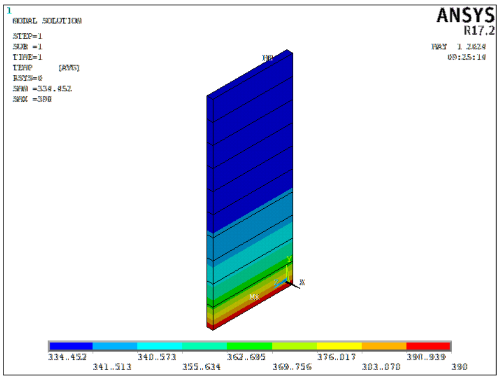

(d) Results.

Figure (4): Steps of the Numerical Model Using ANSYS APDL Software.

c-) Homogenous Model of FG Fin:

From Figure (4-a) and equation (10), the equivalent properties of FG fin can be calculated using the following equation [22,23]:

$$\sum_{i=1}^{10}\left(\frac{\Delta L}{\lambda_i}\right)=\frac{L}{\lambda_{eq}}$$

$$\therefore \lambda_{eq}=\frac{L}{\sum_{i=1}^{10}\left(\frac{\Delta L}{\lambda_i}\right)} \qquad \ldots(11)$$

Where:(λ_i)Is the property of i-th part, and (λ_{eq})It is the equivalent property.

This work calculates the equivalent thermal conductivity of FG fins for each property ratio (f) factor and linear equation slope. (τ) And then, it is used to calculate the temperature distribution of homogenous fins using equation (9').

4. Cases Studied:

In this work, the effect of slop of linear equation (τ), a factor of property ratio (*f*) and temperature ratio $\left(\frac{T_\infty}{T_b}\right)$ The distribution of temperature along the length of the FG fin. The cases studied in this work are lists Table (3).

Table (3): The cases examined in this work.

No.	T_∞ (C)	T_b (C)	T_∞/T_b	Material Distribution Type	The factor of Property Ratio (*f*)
1	25	125	0.2	*Case 1*: $k(L) > k(0)$	*f*=0, 0.2, 0.4, 0.5, 0.6, 0.8 and 1
2	25	50	0.5		
3	25	31.25	0.8		
4	25	20	1.25		
5	25	12.5	2		
6	25	6.25	4		
7	25	125	0.2	*Case* 2: $k(0) > k(L)$	*f*=0, 0.2, 0.4, 0.5, 0.6, 0.8 and 1
8	25	50	0.5		
9	25	31.25	0.8		
10	25	20	1.25		
11	25	12.5	2		
12	25	6.25	4		

5. Results and Discussion:

5.1 Check Accuracy:

This section studies the accuracy of the ANSYS and equivalent properties models compared with the analytical solution. Figure (5) demonstrates the comparison between the temperature calculated by analytical, equivalent property and ANSYS models for different ($T\infty/Tb$) and various values of factor of property ratio (f=0,0.5 and 1) at η=0.5 and η=1 when k(L)>k(0). When (f=0) (i.e., homogenous material), the temperatures of the analytical solution at any point are the same in the equivalent property model. But the difference between them appears when the factor of property ratio(f) increases (i.e. when the ratio (k(L)>k(0)) increases). On the other hand, the results of the ANSYS model behave as lower than the analytical values for a lower $T\infty/Tb$ ratio. In comparison, the numerical results become higher for the higher $T\infty/Tb$ ratio for both η=0.5 and η=1. The maximum absolute percentage of error between analytical results and equivalent property results is (2.363%) when (η=0.5), (f=0.5), and ($T\infty/Tb$=0.2). The maximum absolute percentage of error between analytical results and ANSYS results is (6.756%) when (η=0.5), (f=1), and ($T\infty/Tb$=0.2), as listed in Table (4).

5.2 Effect of ($T\infty/Tb$) Ratio:

Figure (6) shows the effect of the ($T\infty/Tb$) ratio on the temperature profile along the length of FG fin for different factors of property ratio (f) when k(L)>k(0) (i.e., Case 1). When ($T\infty/Tb$) is smaller than unity (i.e., cooling process), Temperature reduction occurs along the length of the FG fin. But when ($T\infty/Tb$) is more significant than unity (i.e., Heating process), the temperature rises along the FGM fin's length. When η=0 (i.e., at the FG fin base), the input temperature decreases with increasing ($T\infty/Tb$) ratio; in this case, the effect of FG material does not appear. But when (η>0), the effect of FG material starts, and the maximum impact appears when η=1, as illustrated in Figure (7).

When k(0)>k(L) (i.e., Case 2), the effect of the ($T\infty/Tb$) Ratio on the temperature profile along the length of FG fin for different factors of property ratio (f) is illustrated in Figure (8). Similar to Case 1, the temperature increases when ($T\infty/Tb$) is more significant than unity along the FG fin length. Also, the temperature decreases along the length of FG fin if ($T\infty/Tb$) is smaller than unity. If (η>0), the effect of FG material appears, and the maximum effect is found when η=1, as illustrated in Figure (9).

5.3 Effect of Factor of Property Ratio (f):

In this section, the property ratio (f) factor controls the slope of the material properties without changing the parent's materials of the FG fin. The unity value of factor of property ratio (f) means that the material at the base of FG fins is (k_0) ($k_{Alumina}$ in case 1) and the material at the end of FG fins is (k_L) (k_{Copper} in case 1). While the (0.5) value of property ratio (f) means that the material at the base of FG fins is still (k_0) ($k_{Alumina}$ in case 1), but the material at the end of FG fins is (k_L) (0.5 k_{Copper} in case 1). In Figures (6-9), the temperature at the FG fin end reduces with the increasing factor of property ratio (f) at ($T\infty/Tb$) Ratio smaller than unity and for cases (1) and (2). On the other side, at the end of the FG fin, the temperature rises with the increasing factor of property ratio (f) when the ($T\infty/Tb$) Ratio is more significant than unity for cases (1) and (2).

5.4

5.5 Comparison Between Case (1) and (2):

Figure (10) shows the comparison between the temperature of the two cases at the end of FG fin due to (a) the factor of property ratio (f) (see Figure (10-a)) and (b) temperature ratio ($T\infty/Tb$) (see Figure (10-b)). The increase in temperature of the case (1) is more significant than that of case (2), especially at a smaller temperature ratio ($T\infty/Tb$=0.2) and at the maximum factor of property ratio (f=1). This appears sharply in Figures (11 and 12).

At η=0.5

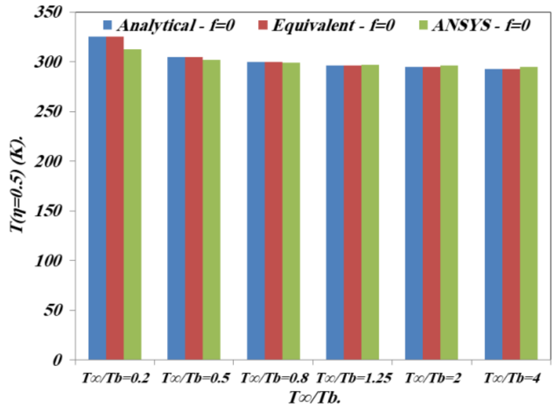

At η=1

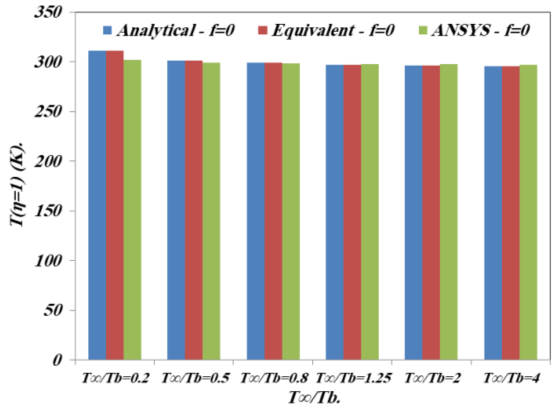

f=0

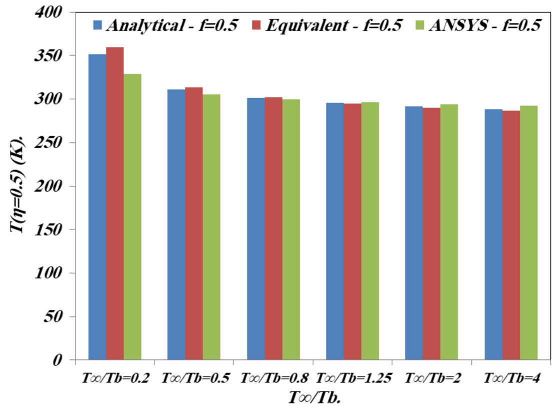

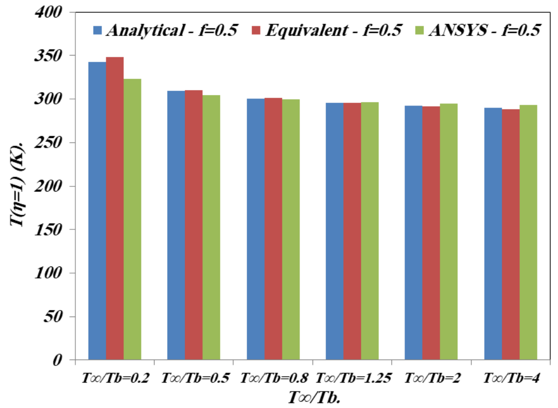

f=0.5

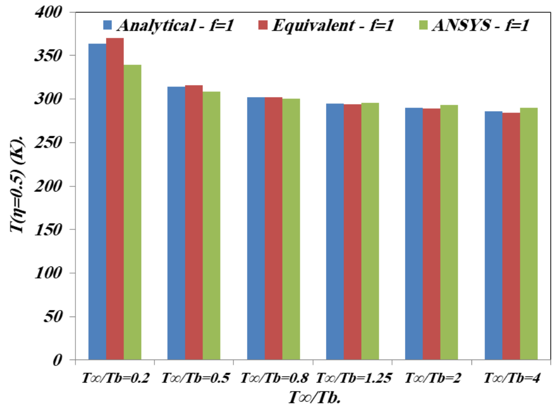

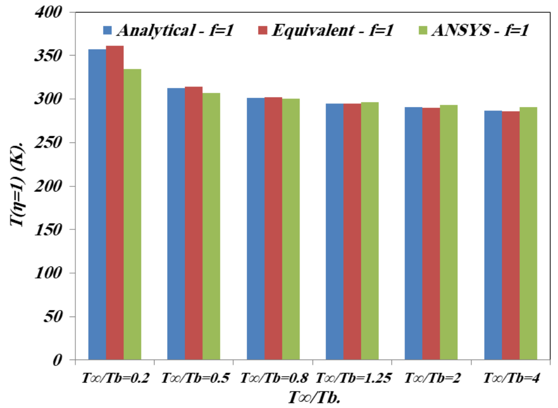

f=1

Figure (5): A Comparison of temperatures determined using analytical, numerical, and equivalent property models of (T_∞/T_b) at η=0.5 and η=1 when $k(L) > k(0)$.

Table (4): The error percentage of the ansys model and equivalent property model concerning the analytical solution for three factors of property ratio values (f) when $k(L) > k(0)$

No.	***T∞/Tb***	***percentage error of the equivalent model about the analytical solution***		***Percentage error of the ansys model regarding the analytical solution***	
1- f=0					
No.	***T∞/Tb***	***η=0.5***	***η=1***	***η=0.5***	***η=1***

International Journal of Multiphysics
Volume 18, No. 3, 2024
ISSN: 1750-9548

1	***0.2***	***0***	***0***	***3.780***	***2.837***
2	***0.5***	***0***	***0***	***1.008***	***0.732***
3	***0.8***	***0***	***0***	***0.257***	***0.184***
4	***1.25***	***0***	***0***	***-0.206***	***-0.150***
5	***2***	***0***	***0***	***-0.520***	***-0.374***
6	***4***	***0***	***0***	***-0.786***	***-0.560***
2- f=0.5					
No.	***T∞/Tb***	***η=0.5***	***η=1***	***η=0.5***	***η=1***
1	***0.2***	***-2.363***	***-1.839***	***6.338***	***5.632***
2	***0.5***	***-0.667***	***-0.509***	***1.788***	***1.559***
3	***0.8***	***-0.172***	***-0.131***	***0.461***	***0.402***
4	***1.25***	***0.141***	***0.106***	***-0.376***	***-0.326***
5	***2***	***0.356***	***0.269***	***-0.957***	***-0.824***
6	***4***	***0.541***	***0.407***	***-1.450***	***-1.249***
3- f=1					
No.	***T∞/Tb***	***η=0.5***	***η=1***	***η=0.5***	***η=1***
1	***0.2***	***-1.767***	***-1.292***	***6.756***	***6.320***
2	***0.5***	***-0.511***	***-0.369***	***1.953***	***1.804***
3	***0.8***	***-0.133***	***-0.096***	***0.509***	***0.467***
4	***1.25***	***0.109***	***0.078***	***-0.416***	***-0.383***
5	***2***	***0.277***	***0.198***	***-1.061***	***-0.969***
6	***4***	***0.422***	***0.301***	***-1.611***	***-1.473***

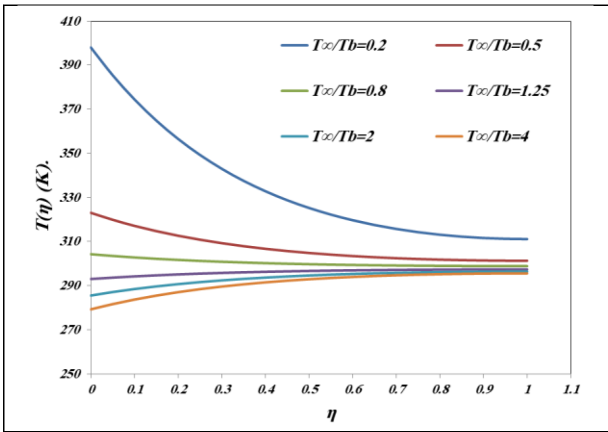

f=0

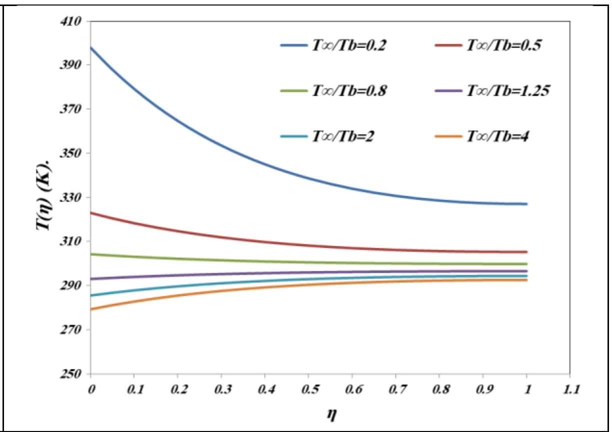

f=0.2

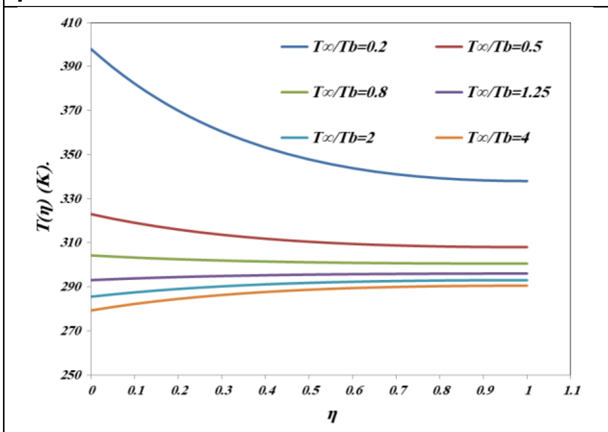

f=0.4

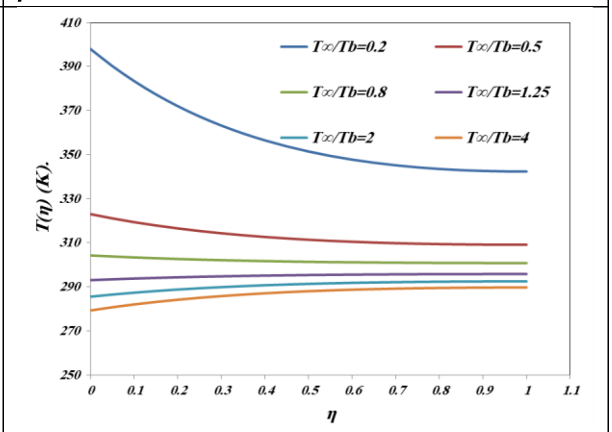

f=0.5

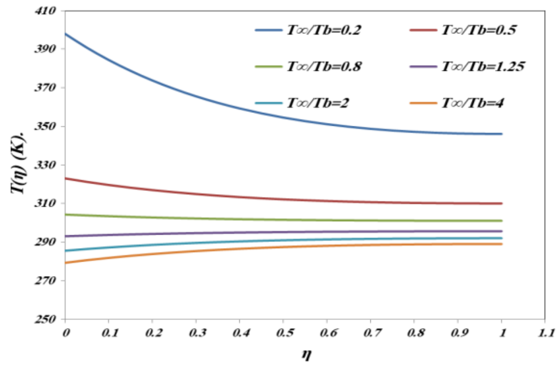

f=0.6

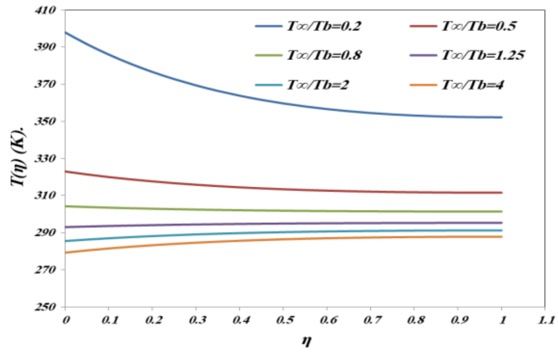

f=0.8

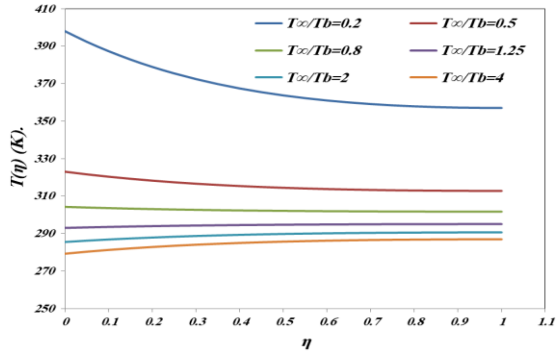

f=1

Figure (6): Temperature profiles comparison for different (t∞/tb) ratios and different factors of property ratio (f) when k(L)>k(0).

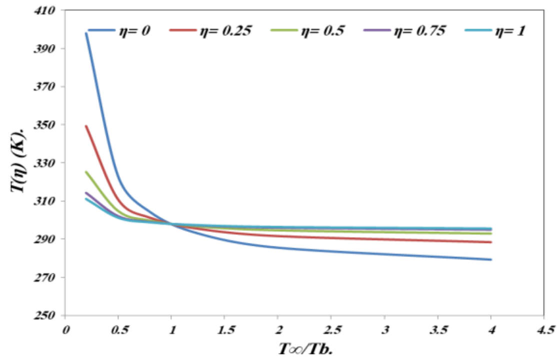

f=0

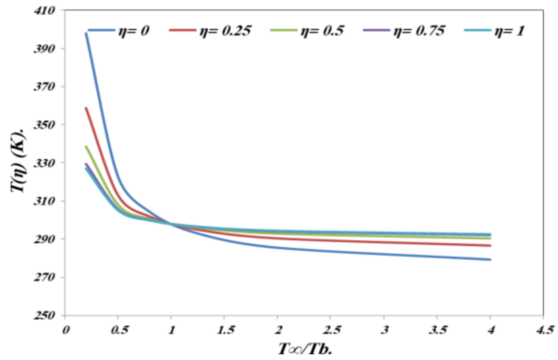

f=0.2

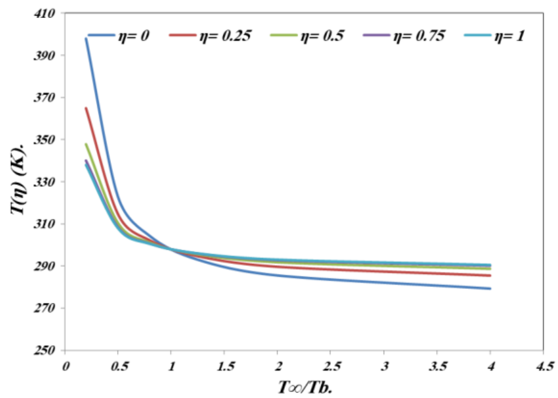

f=0.4

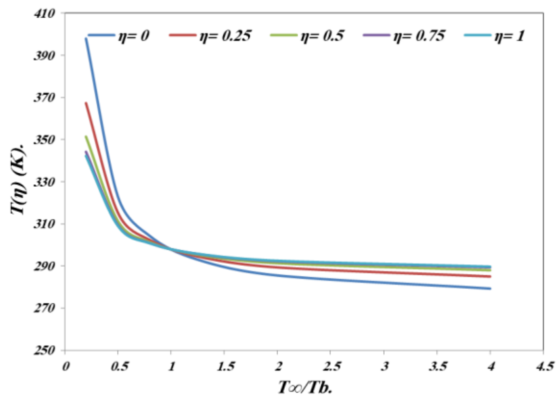

f=0.5

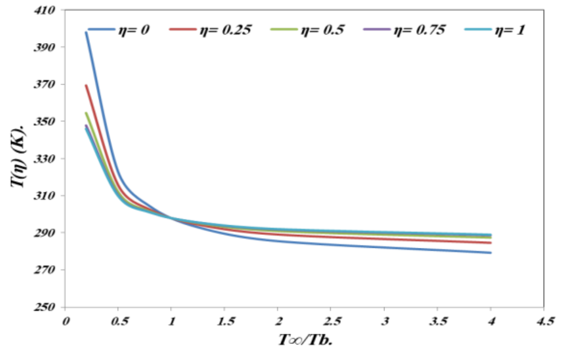

f=0.6

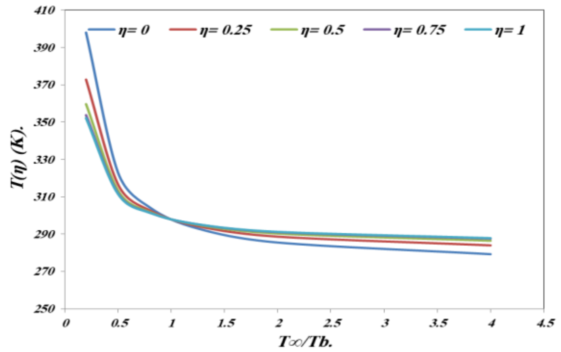

f=0.8

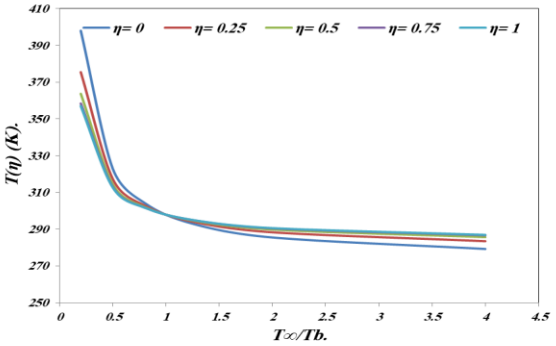

f=1

Figure (7): Comparison of Temperature Variation Due to Increasing (T∞/Tb) Ratio for Different Position (η) and Different Factors of Property Ratio (f) When k(L)>k(0).

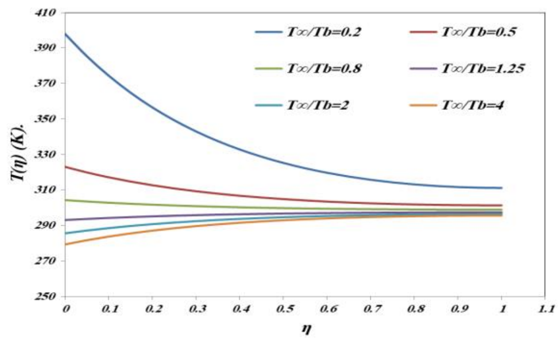

f=0

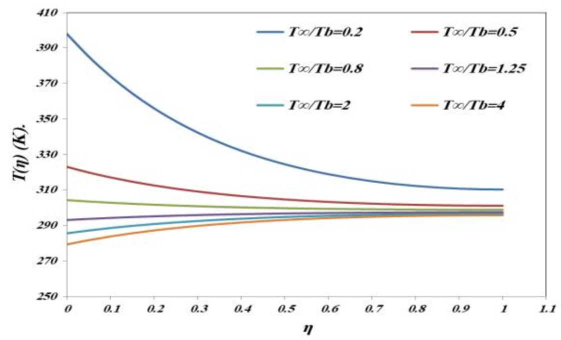

f=0.2

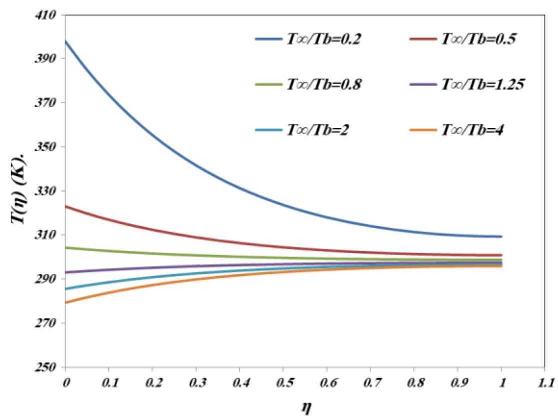

f=0.4

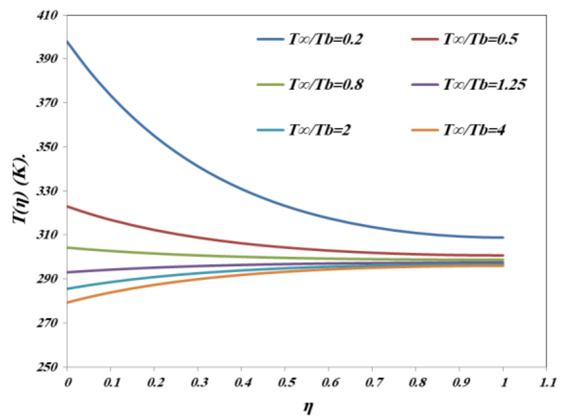

f=0.5

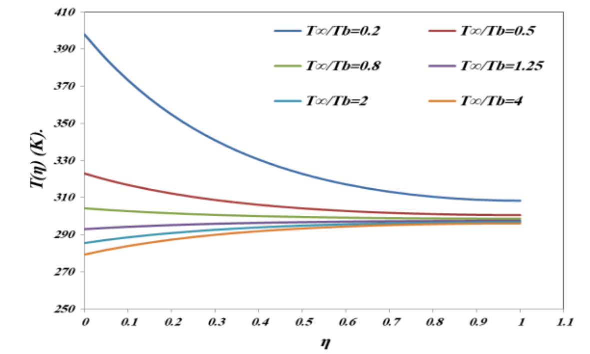

f=0.6

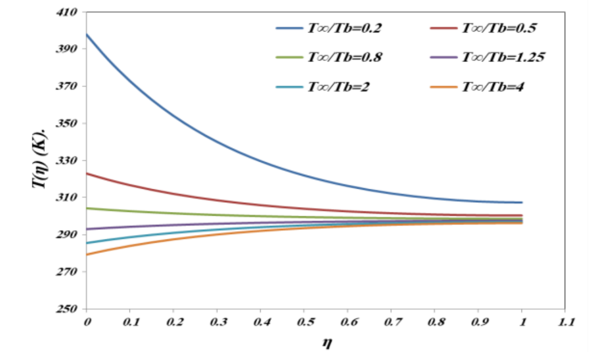

f=0.8

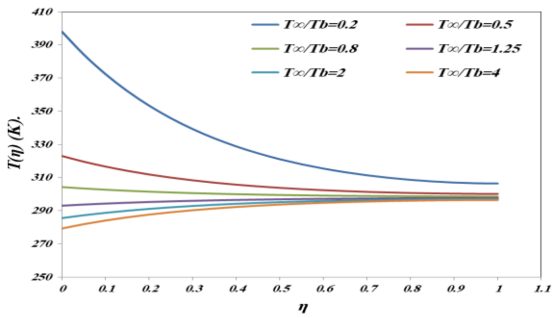

f=1

Figure (8): Temperature distribution comparison for different (t∞/tb) ratios and different factors of property ratio (f) when k(0)>k(L).

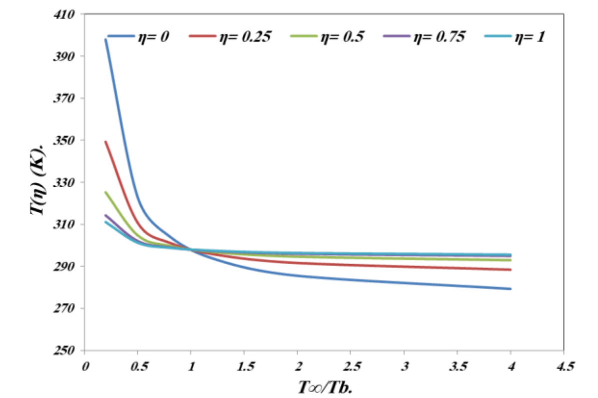

f=0

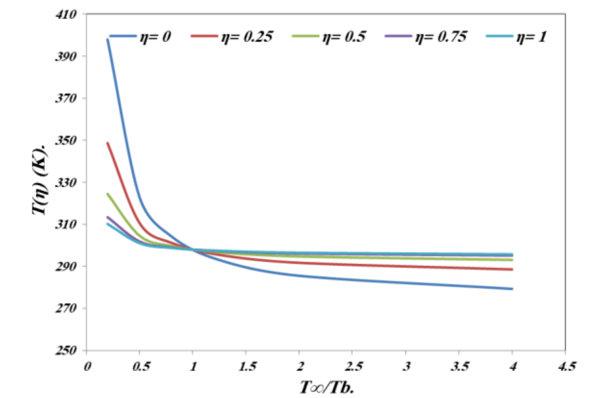

f=0.2

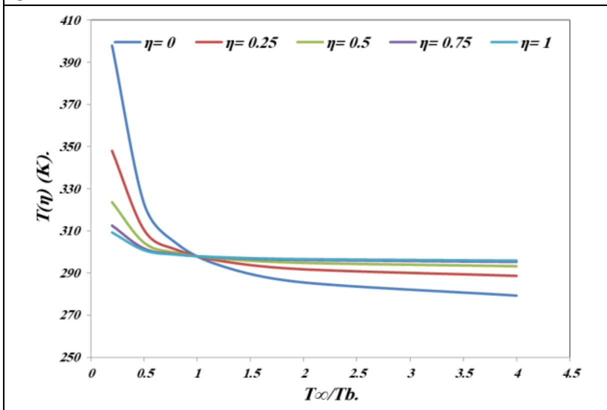

f=0.4

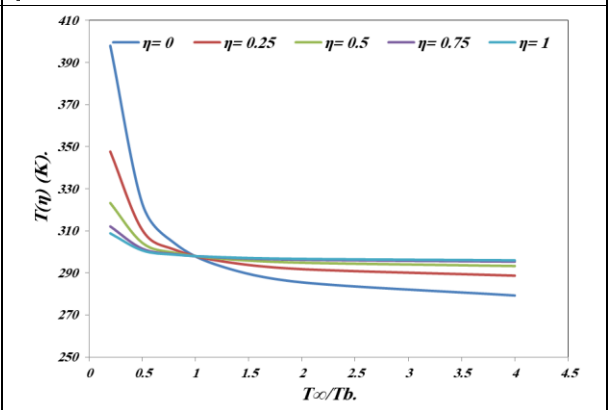

f=0.5

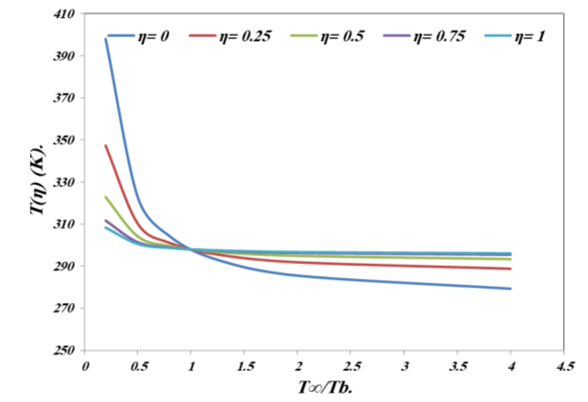

f=0.6

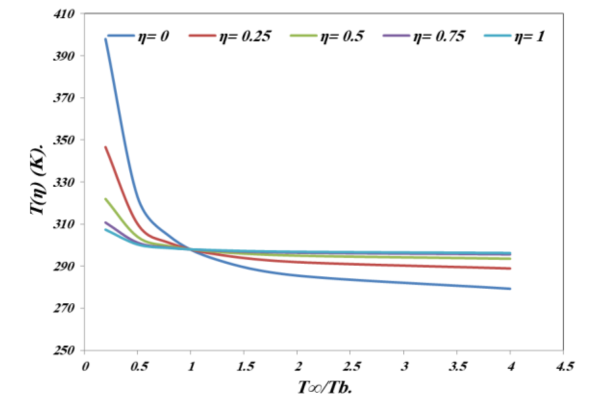

f=0.8

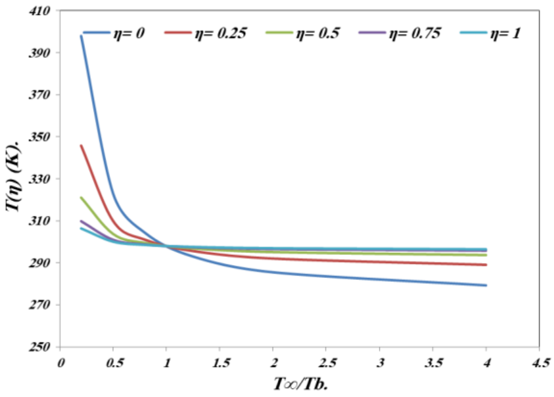

f=1

Figure (9): Comparison of temperature variation due to increasing (t∞/tb) ratio for different positions (η) and various factors of property ratio (f) when k(0)>k(L).

Case 1

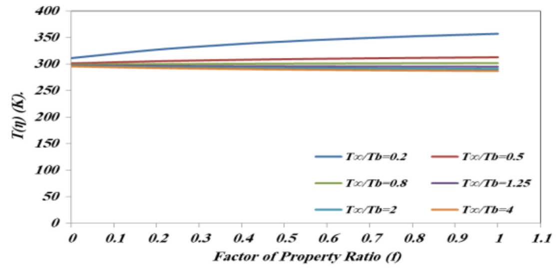

Case 2

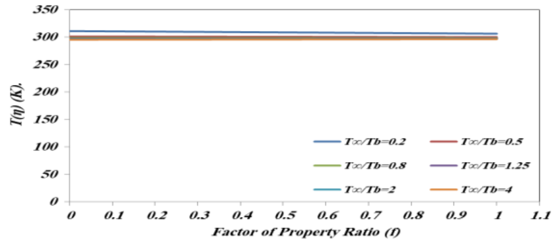

(a) Temperature at the end of FG fin T(η=1) vs. factor of property ratio (f)

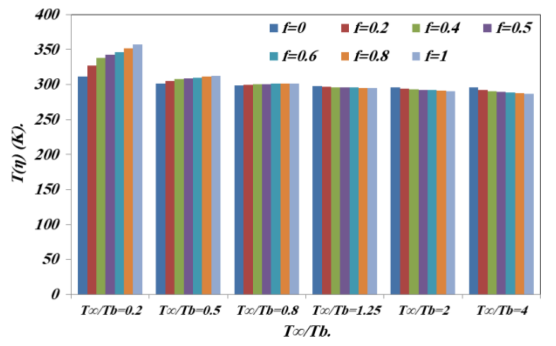

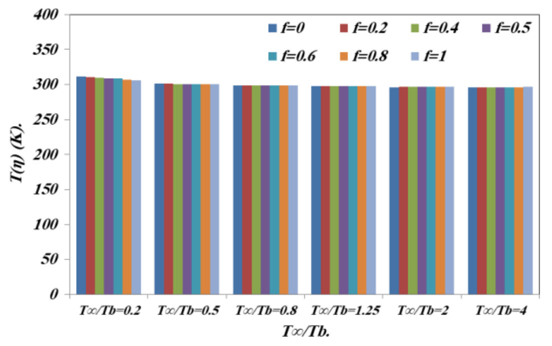

(b) Temperature at the end of fg fin T(η=1) vs. Temperature ratio (T_∞/T_b)

Figure (10) : Comparison between the temperature at the end of fg fin for the two cases.

International Journal of Multiphysics
Volume 18, No. 3, 2024
ISSN: 1750-9548

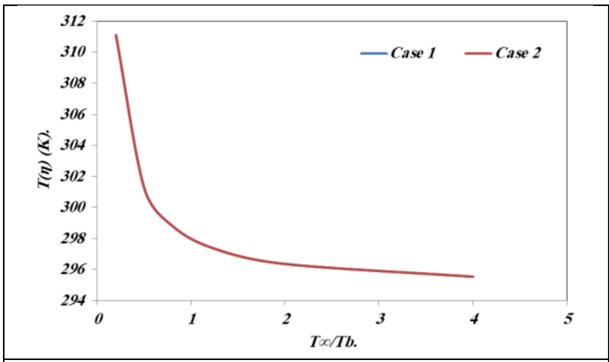

f=0

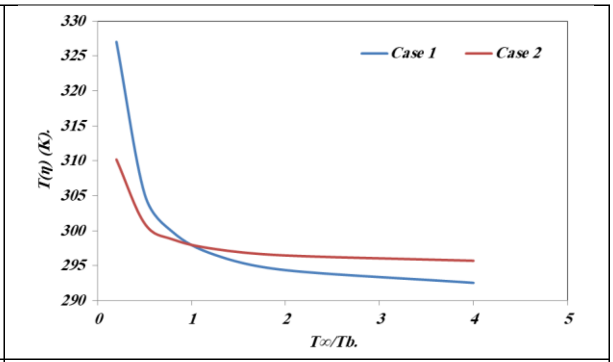

f=0.2

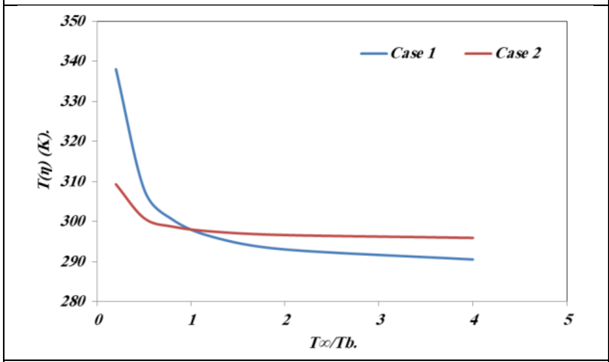

f=0.4

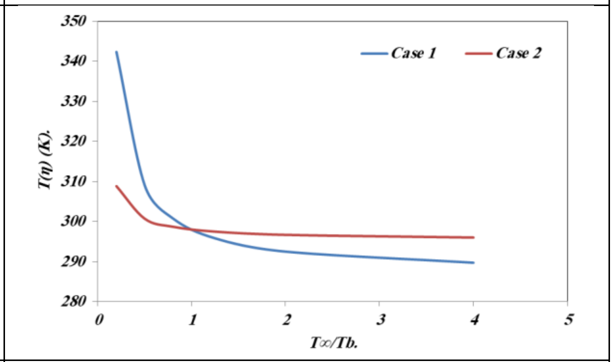

f=0.5

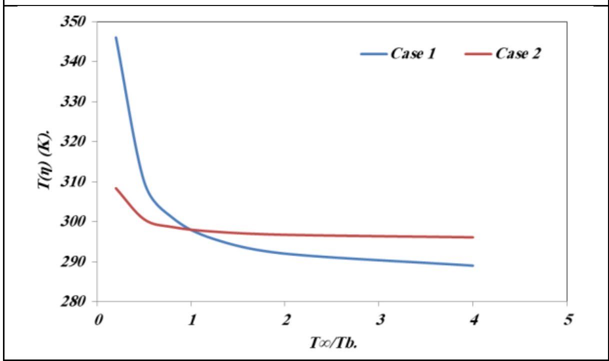

f=0.6

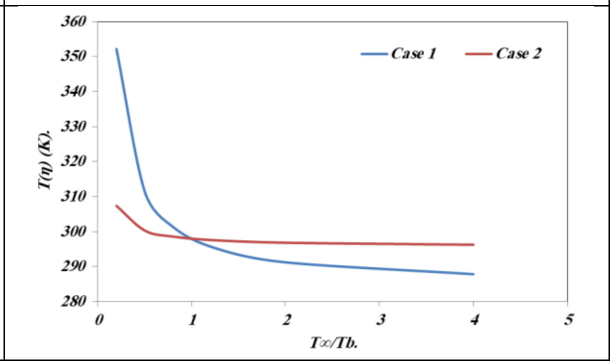

f=0.8

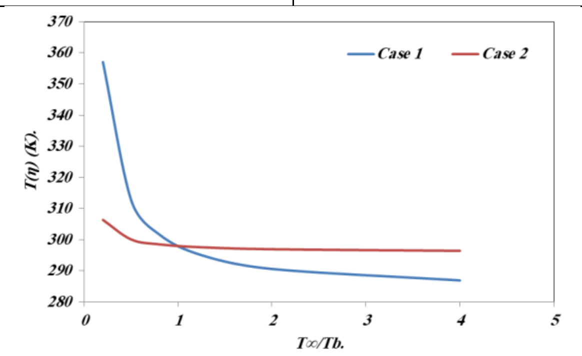

f=1

Figure (11): A comparison of the temperature at the terminus of the fg fin in two cases in which the temperature ratio was increased (T∞/Tb) for different factors of property ratio (f).

International Journal of Multiphysics
Volume 18, No. 3, 2024
ISSN: 1750-9548

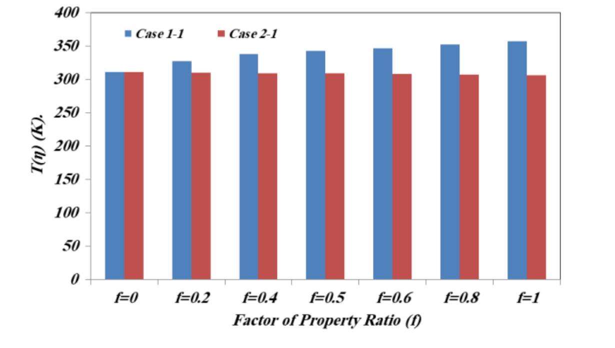

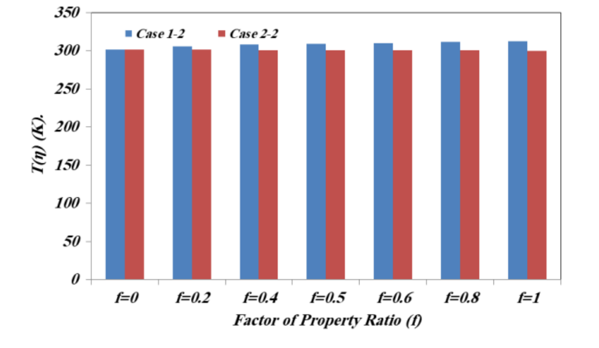

T∞/Tb=0.2 **T∞/Tb=0.5**

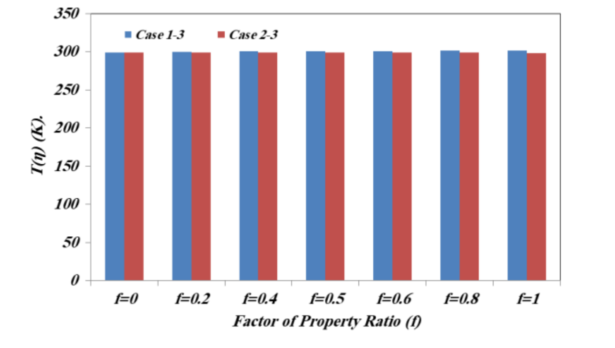

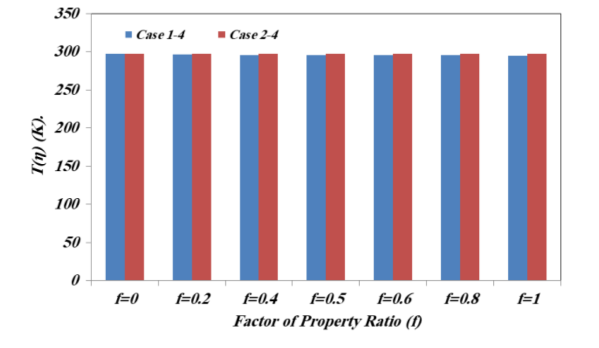

T∞/Tb=0.8 **T∞/Tb=1.25**

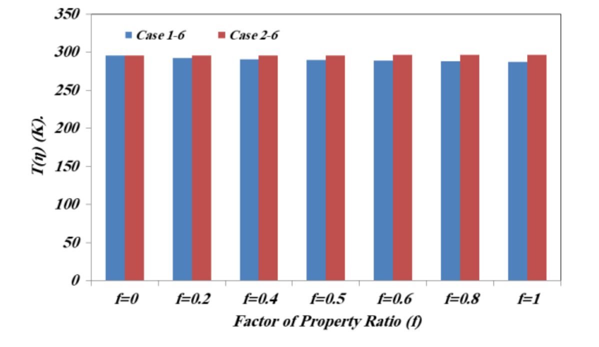

T∞/Tb=2 **T∞/Tb=4**

Figure (12): Comparison between the temperature at the end of fg fin for the two cases due to the increased factor of property ratio (f) for different temperature ratios (T∞/Tb).

6. Conclusions and Future Works:

The current study has presented Numerical and analytical work to investigate the thermal performance of FGM-based fins. Thermal properties of the FGM-based fins are assumed to be changed linearly along the fin's length. Equivalent properties of the fin's material have also been considered in the current work. The number of remarks concluded from the present study:

1- As thermal conductivity increases along the fin's length (k(L)>k(0)), for lower *f*, the result in the case of equivalent properties is like the results in the case of the analytical solution. At the same time, the difference appears as *f* increases.

2- In the case of (k(L)>k(0)), as the (T∞/Tb) ratio is lower than 1 (cooling process), the numerical results become lower than the analytical results and vice versa in the case of (T∞/Tb) ratio higher than 1 (heating process. The maximum error between both solutions is (6.756%) when (η=0.5), (*f*=1), and (T∞/Tb=0.2), while the maximum error between results in cases of numerical and equivalent properties is (2.363%) when (η=0.5), (*f*=0.5) and (T∞/Tb=0.2).

3- In the case of k(L)>k(0), as (T∞/Tb ratio) is lower than unity (cooling process), the increase in (*f*) leads to a rise in the local fin's temperature. In contrast, a slight reduction in the fin's temperature happens as the T∞/Tb ratio becomes higher than unity (heating process). This means that FGM material acts as a barrier against thermal shock.

4- In k(L)>k(0), the (*f*) factor affects the temperature changes along the fin's length very slightly. This conclusion is expected as thermal conductivity decreases along the fin's length affecting the heat transfer along the fin by conduction negatively.

Overall, it can be concluded that the performance of the FGM-based fins is better than the regular based fins thermally.

Acknowledgment

This work was supported partially by the faculty of engineering at the University of Kufa. The authors are very thankful for this support.

References

[1] Akinbowale T. Akinshilo, Analytical Decomposition Solutions for Heat Transfer on Straight Fins with Temperature-Dependent Thermal Conductivity and Internal Heat Generation, Journal of Thermal Engineering, Yildiz Technical University Press, Istanbul, Turkey. 5 (1) (2019) 76-92.

[2] JH Tian, K. Jiang, Heat conduction investigation of the functionally graded materials plates with variable gradient parameters under exponential heat source load, International Journal of Heat and Mass Transfer 122 (2018) 22–30.

[3] Z. Zhong, L.Z. Wu, W.Q. Chen, Progress in the study on mechanics problems of functionally graded materials and structures, Adv. Mech. 40 (5) (2010) 528–541.

[4] Gaba VK, AK Tiwari, S Bhowmick , Performance of Functionally Graded Exponential Annular Fins of Constant Weight, Advances in Functionally Graded Materials and Structures, 2016.

[5] Oguntala GA, Sobamowo GM, Abd-Alhameed, Numerical study of performance of porous fin heat sink of functionally graded material for improved thermal management of consumer electronics. IEEE Transactions on Components, Packaging and Manufacturing Technology. 9(7) (2019) 1271-1283.

[6] Khan W. A. and Aziz A., Transient heat transfer in a functionally graded convecting longitudinal fin, Heat Mass Transfer 48 (2012) 1745–1753.

[7] Hassanzadeha R. and Bilgili M., assessment of thermal performance of functionally graded materials in longitudinal fins, Journal of Engineering Physics and Thermophysics, 91 (2018) 79-88.

[8] Jemiseye Akinwale Emmanuel, Gbeminiyi Musibau Sobamowo, Olayiwola Olatunji Mayowa, Transient Thermal Cooling of Electronics Systems using Functional Graded Fins: Hybrid Computational Analysis, The Journal of Engineering and Exact Sciences, 09 (04) (2023) 1-15.

[9] Sobamowo M. G., G. A. Oguntala, and A. A. Yinusa, Nonlinear Transient Thermal Modeling and Analysis of a Convective-Radiative Fin with Functionally Graded Material in a Magnetic Environment, Modelling and Simulation in Engineering Volume (2019) 1-16.

[10] Hassanzadeh Rahim, Bilgili Mehmet, Improvement of thermal efficiency in computer heat sink using functionally graded materials, Communications on Advanced Computational Science with Applications, (2014) 1-13.

[11] Ranjana R., and Mallick A., An Efficient Unified Approach for Performance Analysis of Functionally Graded Annular Fin with Multiple Variable Parameters, Thermal Engineering, 65 (9) (2018) 614–626.

[12] George Oguntala, Isah Danjuma, Gbeminiyi Sobamowo, Raed Abd-Alhameed & Jim Noras, Nonlinear Thermal Analysis of a Convective-Radiative Longitudinal Porous Fin of Functionally Graded Material for Efficient Cooling of Consumer Electronics, International Journal of Ambient Energy, 43(1) (2019) 385–399.

[13] Kumar, C.; Nimmy, P.; Nagaraja, KV; Kumar, R.S.V.; Verma, A.; Alkarni, S.; Shah, N.A. Analysis of Heat Transfer Behavior of Porous Wavy Fin with Radiation and Convection by Using a Machine Learning Technique. Symmetry 15 (2023) 1601.
[14] Oguntala G, Sobamowo G, Ahmed Y. Transient analysis of functionally graded material fin under the effect of Lorentz force using the integral transform method for improved electronic packaging. Heat Transfer, 49 (2020) 2627–2644.
[15] Sobamowo, M.G, M. O. Salami, A. O. Yinusa, E. H. Abubakar, Finite Element Analysis of Transient Thermal Behavior of Radiative-Convective Fin with Functionally Graded Material under the Influence of Magnetic Field, Journal of Complex Flow, 5 (1) (2023) 31-38.
[16] Raghad Azeez Neamah, Ameen Ahmad Nassar and Luay S. Alansari, Modeling and Analyzing the Free Vibration of Simply Supported Functionally Graded Beam, J. Aerosp. Technol. Manag. 14 (2022) e1522. https://www.jatm.com.br/jatm/article/view/1264/938. 24-7-2022.
[17] Agata Strojny-Nȩdza, Katarzyna Pietrzak, and Witold Wȩglewski, The Influence of Al2O3 Powder Morphology on the Properties of Cu-Al2O3 Composites Designed for Functionally Graded Materials (FGM), Journal of Materials Engineering and Performance, 25 (8) 2016 DOI: 10.1007/s11665-016-2204-3.
[18] F. P. Incropera, D. P. DeWitt, Introduction to Heat Transfer, Wiley, (2011), 6 edition.
[19] A. Acosta-Iborra, A. Campo, Approximate analytic temperature distribution and efficiency for annular fins of uniform thickness, International Journal of Thermal Science, 48 (2009) 773-780. http://dx.doi.org/10.1016/j.ijthermalsci.2008.05.012
[20] ANSYS help.
[21] Walaa Mohammed Hashim, Luay S. Alansari, Mohanad Aljanabi, and Hassan Mansour Raheem," Investigating Static Deflection of Non-Prismatic Axially Functionally Graded Beam", Hindawi, Material Design & Processing Communications, Volume 2022, Article ID 7436024, 12 pages. https://doi.org/10.1155/2022/7436024.
[22] Turant, J., and Radaszewska, E., "Thermal Properties of Functionally Graded Fibre Material", Fibres & Textiles in Eastern Europe, 24 (4) (2016) 68-73,
[23] Nasr Abdulameer Jabbar; "An Investigation of Thermal-Structural Coupling Problem of Dry Friction Clutches and Environmental Impact"; Ph.D. Thesis 2023, University of Baghdad.